


**Probing the limits of correlations in an indivisible quantum system**M. Malinowski,<sup>1,\*</sup> C. Zhang,<sup>1</sup> F. M. Leupold,<sup>1</sup> A. Cabello,<sup>2</sup> J. Alonso,<sup>1,†</sup> and J. P. Home<sup>1,‡</sup><sup>1</sup>*Institute for Quantum Electronics, ETH Zürich, Otto-Stern-Weg 1, 8093 Zürich, Switzerland*<sup>2</sup>*Departamento de Física Aplicada II, Universidad de Sevilla, 41012 Sevilla, Spain* (Received 22 December 2017; revised manuscript received 6 February 2018; published 16 November 2018)

We employ a trapped ion to study quantum contextual correlations in a single qutrit using the 5-observable Klyachko, Can, Binicioğlu, and Shumovsky inequality, which is arguably the most fundamental noncontextuality inequality for testing quantum mechanics (QM). We quantify the effect of systematics in our experiment by purposely scanning the degree of signaling between measurements, which allows us to place realistic bounds on the nonclassicality of the observed correlations. Our results violate the classical bound for this experiment by up to 25 standard deviations, while being in agreement with the QM limit. In order to test the prediction of QM that the contextual fraction increases with the number of observables, we gradually increase the complexity of our measurements from 5 up to 121 observables. We find stronger-than-classical correlations in all prepared scenarios up to 101 observables, beyond which experimental imperfections blur the quantum-classical divide.

DOI: [10.1103/PhysRevA.98.050102](https://doi.org/10.1103/PhysRevA.98.050102)

Quantum contextuality speaks against the classical perception that the act of measurement merely reveals preexisting, context-independent properties of the measured system. This leads to correlations between observables which are stronger than those in classical physics [1]. One way to test these is to construct noncontextuality (NC) inequalities which are constrained classically but violated by quantum systems. The most famous of those is the Bell inequality on two spacelike separated qubits [2,3]. However, contextuality can be observed already in a single particle. In Ref. [4], Klyachko, Can, Binicioğlu, and Shumovsky (KCBS) provided an inequality with the lowest possible number of measurement settings and the largest possible gap between quantum and classical predictions [5,6]. It requires measuring  $N = 5$  observables in a three-level system or qutrit, the smallest quantum state space in which such correlations can be observed. Beyond the minimal instances, both the Bell and KCBS inequalities have been generalized to larger numbers of observables [7].

In addition to demonstrating nonclassicality, the exact value of contextual witnesses is of interest for many applications, such as certifying randomness [8] or constraining the predictive power of beyond-quantum theories. Besides practical uses, it is also interesting how close one can get to the bounds imposed by the quantum theory. For such quantitative purposes, the KCBS scenario and its multiobservable generalization are particularly important, since they can exhibit correlations stronger than those available to any other contextual scenario, including Bell tests (see detailed arguments in [6,9]). Furthermore, it was recently shown that a quantity called contextual fraction (CF) measures the amount of computational power available in a quantum system in certain tasks [10]. We will show that as the number of observables

$N$  in the generalized KCBS scenario increases, CF is expected to approach unity, which hints at potential large computational power.

While experiments have already violated NC inequalities in both Bell [11–13] and KCBS [6,14] scenarios, the legitimacy of quantitative test of correlations has recently been challenged based on signaling [15]. There is signaling between two measurements  $M_1$  and  $M_2$  when, for at least one input state, outcome statistics of  $M_2$  indicate whether or not  $M_1$  was performed before. This is a “red flag” that the assumption of compatible measurements, which underlies the theory, has been violated. Tests aiming at saturating the (Tsirelson) quantum bound of the Bell inequality [16,17] have been called into question because of this issue [15], and all existing KCBS tests show signaling as well [6]. Given that NC inequalities can show a trade-off between signaling and the amount of violation, thoroughly accounting for the former is a major pending task and a subject of ongoing theoretical efforts [18,19]. As a consequence, there is no undisputed experimental evidence to date that the maximum predicted by quantum mechanics (QM) for any NC inequality can be reached [6,15]. Furthermore, while generalized Bell inequalities (or Bell chained inequalities) have been violated for up to  $N = 90$  observables [17,20], existing tests of the generalized KCBS scenario, where even stronger correlations are possible, are limited to  $N \leq 7$  [21].

In this Rapid Communication, we present experimental results which reach the QM bound of the KCBS inequality, and which exhibit correlations beyond those accessible in a Bell experiment [6,9]. We also extend the KCBS test to  $5 \leq N \leq 121$  and perform a measurement of the contextual fraction in an indivisible system. We measure stronger-than-classical correlations up to  $N = 101$  observables and the largest CF = 0.800(4) for  $N = 31$  [22]. We examine the assumptions of compatible measurements [15,23] by purposely scanning the degree of signaling in the experiment, thereby evaluating the trade-off between signaling and violation in NC inequalities.

\*maciejm@phys.ethz.ch

†alonso@phys.ethz.ch

‡jhome@phys.ethz.ch

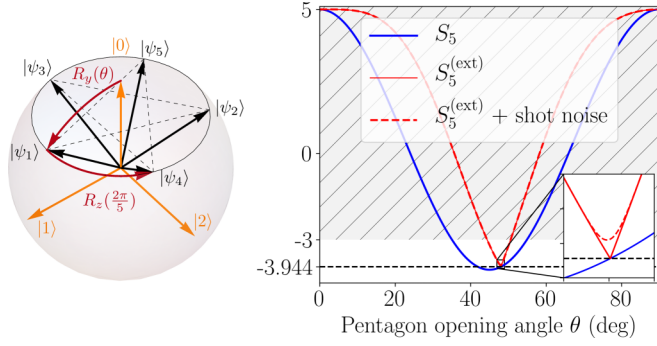


FIG. 1. Left: “Qutrit sphere” spanned by arbitrary superpositions of the type  $\alpha|0\rangle + \beta|1\rangle + \gamma|2\rangle$ , where  $\alpha, \beta, \gamma \in \mathbb{R}$  and such that  $\alpha^2 + \beta^2 + \gamma^2 = 1$ . The directions along which projective measurements are performed are indicated by states  $|\psi_i\rangle$ . When  $\theta = \theta_5$ , states connected by dashed lines are orthogonal. Experimentally relevant rotations are shown in dark red (see text). Right: Predicted values of  $S_5$  [Eq. (2)] and  $S_5^{(\text{ext})}$  [Eq. (4)] as a function of  $\theta$ . The hashed region above  $-3$  shows the space where  $S_5^{(\text{ext})}$  is consistent with NC models. The inset shows how a finite number of experiments (here  $5 \times 10^4$  per data point) leads to a necessary deviation from theory around  $\theta_5$  (dashed line). The analytical formulas for the plotted curves are given in [6].

This allows us to quantify and minimize systematic effects, which we use to penalize our results in line with recent theoretical proposals [19]. In these experiments we combine high-fidelity unitary operations with high-precision projective detection [24] to close both the individual-existence loophole (by performing sequential, rather than simultaneous, measurements [23,25]) and the detection loophole.

We encode the qutrit basis states  $|0\rangle, |1\rangle, |2\rangle$  onto internal electronic energy levels of a single  $^{40}\text{Ca}^+$  ion confined in a cryogenic surface-electrode radio-frequency trap. Combinations of coherent laser pulses resonant with  $|0\rangle \leftrightarrow |1\rangle$  and  $|0\rangle \leftrightarrow |2\rangle$  transitions allow us to generate arbitrary single-qutrit rotations. Quantum nondemolition measurements of arbitrary observables are achieved with high fidelity by combining these coherent rotations with discrimination of  $|0\rangle$  from  $|1\rangle$  or  $|2\rangle$  using state-dependent fluorescence, allowing the study of correlations between sequential measurements [24]. Further details about the encoding, manipulation, and detection of the qutrit are given in [6].

In a first set of experiments we perform sequences of pairs of measurements along rays defined by a set of  $N = 5$  states  $|\psi_i\rangle$  on a “qutrit sphere” of real superpositions of the basis states (see Fig. 1). Explicitly, the *pentagon states* are given by

$$|\psi_i\rangle = U_i|0\rangle \quad \text{with} \quad U_i = R_z^{2i-2}\left(\frac{2\pi}{5}\right)R_y(\theta), \quad (1)$$

where  $R_y(\theta)$  represents a rotation by angle  $\theta$  around  $|2\rangle$  (associated with the  $y$  axis), and  $R_z(\frac{2\pi}{5})$  represents a rotation by angle  $\frac{2\pi}{5}$  around  $|0\rangle$  (associated with the  $z$  axis; Fig. 1). Here  $i$  is a modulo 5 integer, with  $|\psi_0\rangle \equiv |\psi_5\rangle$  and  $|\psi_6\rangle \equiv |\psi_1\rangle$ . We define the measurement along direction  $|\psi_i\rangle$  with outcome  $A_i$  as  $M_i = 2|\psi_i\rangle\langle\psi_i| - 1$ . This means that if the measurement outcome is  $A_i = 1$ , the state is projected onto  $|\psi_i\rangle$ , whereas  $A_i = -1$  projects onto an orthogonal space spanned by  $|\psi_{i-1}\rangle$  and  $|\psi_{i+1}\rangle$ , preserving the coherence

in that subspace [6]. When measurements of  $M_i$  and  $M_j$  are conducted sequentially, with  $M_i$  measured first and  $M_j$  measured second, we denote their respective outcomes as  $A_i^{(1)}$  and  $A_j^{(2)}$ . Projective measurements are compatible when their operators commute ( $[M_i, M_j] = 0$ ).

The KCBS scenario, in which measurements  $M_i$  and  $M_{i\pm 1}$  are compatible, arises when  $\theta_5 = \arccos(5^{-1/4}) \approx 48^\circ$  and hence  $\langle\psi_i|\psi_{i\pm 1}\rangle = 0$ . In Fig. 1, this is indicated by dashed lines joining pairs of states. In NC models the sum of correlators is bounded from below:

$$S_5(\theta_5) = S_5^\pm(\theta_5) = \sum_{i=1}^5 \langle A_i^{(1)} A_{i\pm 1}^{(2)} \rangle \geq \bar{S}_5^{\text{NC}} = -3. \quad (2)$$

This result is called the KCBS inequality [4] in either “normal order” ( $S_5^+$ ) or “reverse order” ( $S_5^-$ ). According to QM,

$$S_5(\theta_5) \geq \bar{S}_5^{\text{QM}} = 5 - 4\sqrt{5} \approx -3.944. \quad (3)$$

This is independent of the order and the equality is obtained if and only if the system is initialized to  $|0\rangle$ .

Note that miscalibration of the opening angle  $\theta$  may result in  $S_5(\theta) < \bar{S}_5^{\text{QM}}$  (see Fig. 1). Such results do not reveal non-classical effects, since outcomes of noncompatible measurements can in general be explained by NC models. However, unavoidable experimental imperfections will always lead to some degree of incompatibility. This fact has been identified as the main weakness of contextuality tests in local systems and is often referred to as the “compatibility” or “finite-precision loophole” [26].

The loophole can be addressed by making use of “extended inequalities” [19,23]. These are modifications of NC inequalities that do not require perfect compatibility. Such inequalities have been used in previous experiments [25,27], but they only allowed one to disprove classical models satisfying additional (and often rather arbitrary) assumptions. In contrast, recent approaches extend the traditional notion of contextuality to account for possible experimental imperfections, and still allow one to disprove general NC theories. Notably, within the “contextuality-by-default” framework [19] the KCBS inequality can be extended to

$$S_5^{(\text{ext})}(\theta) = \sum_{i=1}^5 \langle A_i^{(1)} A_{i\pm 1}^{(2)} \rangle + \sum_{i=1}^5 \epsilon_i \geq \bar{S}_5^{\text{NC}} = -3, \quad (4)$$

where  $\epsilon_i = |\langle A_i^{(1)} \rangle - \langle A_i^{(2)} \rangle|$ , and thus  $\sum_{i=1}^5 \epsilon_i$  quantifies signaling between measurements. Note that this inequality can be used for both normal and reverse order measurements. The intuition behind  $\epsilon_i$  is as follows: ideally, the average outcome  $A_i$  of measurement  $M_i$  is the same whether it is performed before ( $\langle A_i^{(1)} \rangle$ ) or after ( $\langle A_i^{(2)} \rangle$ ) another measurement and so  $\epsilon_i = 0$ . Should, however, the first measurement distort the second,  $\langle A_i^{(1)} \rangle \neq \langle A_i^{(2)} \rangle$  and so  $\epsilon_i > 0$ .

$S_5^{(\text{ext})}(\theta)$  is plotted in Fig. 1 (red dashed line), showing that within this extended framework a finite range of  $\theta$  leads to results inconsistent with NC models (hashed region). Aside from systematic effects, some amount of signaling is expected purely due to shot-noise-limited statistics (otherwise known as quantum projection noise). This means that experimental

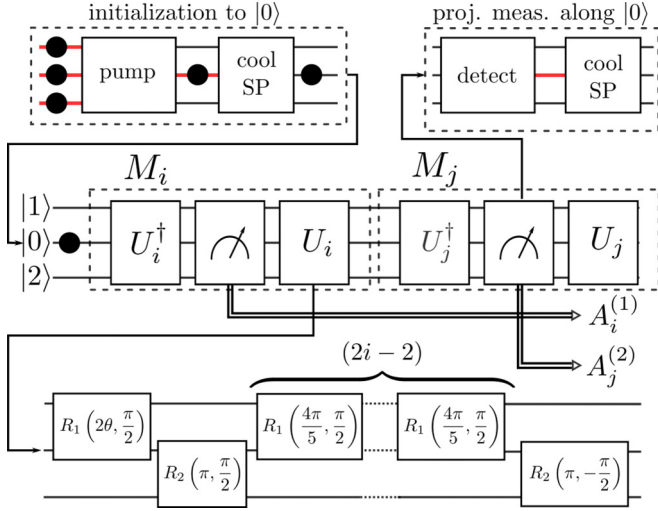


FIG. 2. Sequential measurement of observables  $M_i$  and  $M_j$ . Red lines illustrate the parts of the sequence where the ion is hot and/or outside the computational basis. In the *pump* stage, the ion is Doppler cooled and pumped into the  $S_{1/2}$  manifold, which includes state  $|0\rangle$ . In the *detect* stage, the state is projected either onto the  $\{|1\rangle, |2\rangle\}$  manifold (without affecting its motional state), or onto the  $S_{1/2}$  manifold (heating it back to the Doppler limit). In the *cool SP* stage, the  $S_{1/2}$  states are ground-state cooled and pumped into  $|0\rangle$ , while states  $|1\rangle$  and  $|2\rangle$  remain unaffected. Each unitary  $U_i$  is decomposed into a sequence of  $(2i + 1)$  coherent rotations on  $|0\rangle \leftrightarrow |1\rangle$  and  $|0\rangle \leftrightarrow |2\rangle$  transitions. Every sequence produces outcomes  $A_i^{(1)}$  and  $A_j^{(2)}$ , from which we calculate the correlator  $A_i^{(1)}A_j^{(2)}$ . For every setting, the measurement is repeated 10 000 times.

results are expected to systematically deviate from  $S_5^{(\text{ext})}(\theta)$  for a finite number of measurements (Fig. 1, red dashed line).

All experiments in this work follow the sequence depicted in Fig. 2. We start by cooling the ion's motion close to the ground state to suppress the effect of finite motional temperature on the fidelities of coherent control operations [24]. We then optically pump the system to  $|0\rangle$  and perform a measurement  $M_i$  followed by a measurement of  $M_{j=i\pm 1}$ . Projective measurements along  $|0\rangle$  are performed by applying a fluorescence state-detection pulse, followed by ground-state cooling and optical-pumping pulses [6]. If the ion fluoresces it is projected onto  $|0\rangle$  and cooled back close to the ground state; if it does not, it is projected onto the subspace spanned by states  $|1\rangle$  and  $|2\rangle$ , without affecting their relative amplitudes or the motional state [24]. A projective measurement along  $|\psi_i\rangle = U_i|0\rangle$  is composed of a coherent rotation  $U_i^\dagger$ , followed by a projective measurement along  $|0\rangle$  and a rotation back  $U_i$  [6,24]. This allows us to treat each measurement as a block that is executed in the same way regardless of preceding or following measurements [28]. Qutrit rotations are decomposed into individual laser pulses using Eq. (1), with

$$R_y(\theta) = R_1\left(2\theta, \frac{\pi}{2}\right), \quad (5a)$$

$$R_z^{2i-2}\left(\frac{2\pi}{5}\right) = R_2\left(\pi, \frac{\pi}{2}\right)R_1^{2i-2}\left(\frac{4\pi}{5}, \frac{\pi}{2}\right)R_2\left(\pi, -\frac{\pi}{2}\right), \quad (5b)$$

where  $R_k^n(\theta, \phi)$  ( $k = 1, 2$ ) is a matrix representing the effect of a resonant pulse on the  $|0\rangle \leftrightarrow |k\rangle$  transition with angle  $\theta$

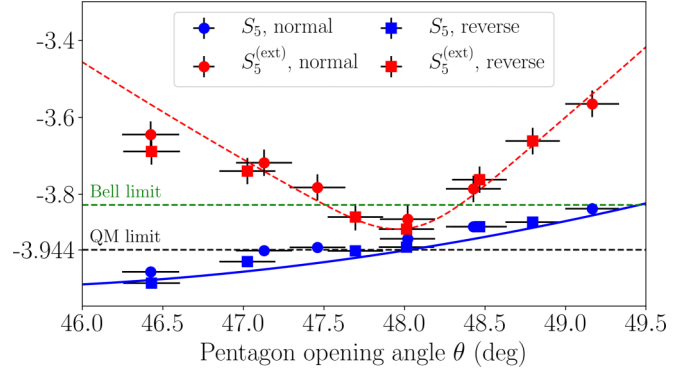


FIG. 3. Results of the KCBS measurement as a function of the opening angle  $\theta$ . Each data point results from 10 000 measurements on each of the five correlators  $\langle A_i A_j \rangle$ , either in normal ( $j = i + 1$ ) or reverse order ( $j = i - 1$ ). Blue and dashed red lines represent theoretical expectations for  $S_5$  and  $S_5^{(\text{ext})}$ , respectively (see Fig. 1, right). Note that all measurements of  $S_5^{(\text{ext})}$  violate the NC bound of  $S_5^{\text{NC}} = -3$ . Error bars here and in the remainder of the Rapid Communication show the standard error in the mean, with sample standard deviation obtained directly from the data [6].

and phase  $\phi$ , repeated  $n$  times [6]. Experimentally, these parameters are adjusted by changing the laser-pulse amplitude, duration, and phase with an acousto-optic modulator.

In the KCBS study we scan the degree of incompatibility between observables by changing the pentagon opening angle  $\theta$  and measuring each pair of observables 10 000 times in both normal and reverse order. We determine the experimental value of  $\theta$  using

$$\theta = \frac{1}{2} \arccos \left( \sum_{i=1}^N \frac{\langle A_i^{(1)} \rangle}{N} \right). \quad (6)$$

The measured witnesses  $S_5(\theta)$  and  $S_5^{(\text{ext})}(\theta)$  are displayed in Fig. 3, together with theoretical expectations for an ideal experiment. Table I shows the results of this procedure for the value of  $\theta$  measured to be closest to  $\theta_5 \approx 48^\circ$  in each scan. The results of  $S_5(\theta_5)$  exhibit a systematic shift of 1.6 standard deviations from the ideal QM prediction. This can be attributed to imperfections in qutrit rotations, primarily due to vibrations of the closed-cycle cryostat where the ion trap sits. For the extended witness  $S_5^{(\text{ext})}(\theta_5)$ , statistical errors dominate. The data point closest to compatibility violates the KCBS inequality (2) by 65 (67) standard deviations in the normal (reverse) order. In addition, all measured data points violate the extended KCBS inequality (4) by up to 25 standard deviations [29].

Recent theoretical developments allow for a unified treatment of different NC inequalities and consequently justify a direct comparison between contextuality and Bell tests [9]. Within the formalism of exclusivity structures [6], KCBS and its generalization (odd  $N$ -cycle NC inequalities [7]) correspond to the most fundamental exclusivity scenarios, which are building blocks of all other NC inequalities. Bell experiments (even  $N$ -cycle NC inequalities) produce correlations that cannot saturate those available due to their exclusivity graph. The largest amount of contextuality available to Bell

TABLE I. Experimental results for the KCBS experiment for the points closest to the compatibility angle  $\theta = \theta_5$  in both normal and reverse order in Fig. 3.

| Order       | $i$   | $j$ | $\langle A_i \rangle$                                   | $\langle A_j \rangle$                               | $\langle A_i A_j \rangle$ |
|-------------|-------|-----|---|---|---------------------------|
| Ideal       |       |     | $\approx -0.105$  | $\approx -0.105$                                    | $\approx -0.788$          |
| Ideal total |       |     | $S_5 \approx -3.944, S_5^{(\text{ext})} \approx -3.888$ |   |                           |
| Normal      | 1     | 2   | -0.106(10)  | -0.107(10)  | -0.786(6)                 |
|             | 2     | 3   | -0.111(10)  | -0.092(10)  | -0.793(6)                 |
|             | 3     | 4   | -0.107(10)  | -0.112(10)  | -0.775(6)                 |
|             | 4     | 5   | -0.102(10)  | -0.107(10)  | -0.787(6)                 |
|             | 5     | 1   | -0.100(10)  | -0.121(10)  | -0.774(6)                 |
|             | Total |     |   | $S_5 = -3.915(14), S_5^{(\text{ext})} = -3.864(34)$ |                           |
| Reverse     | 1     | 2   | -0.113(10)  | -0.096(10)  | -0.786(6)                 |
|             | 2     | 3   | -0.111(10)  | -0.101(10)  | -0.787(6)                 |
|             | 3     | 4   | -0.106(10)  | -0.103(10)  | -0.784(6)                 |
|             | 4     | 5   | -0.093(10)  | -0.118(10)  | -0.783(6)                 |
|             | 5     | 1   | -0.102(10)  | -0.097(10)  | -0.798(6)                 |
|             | Total |     |   | $S_5 = -3.937(14), S_5^{(\text{ext})} = -3.890(34)$ |                           |

scenarios would correspond to  $S_5 \approx -3.828$  (green dashed line in Fig. 3, [6]). Close to compatibility we can resolve values of  $S_5$  surpassing this bound.

In a second set of experiments we expand the above procedure to correlation measurements between any odd number  $N > 5$  of states on the ‘‘qutrit sphere.’’ Generalizing the KCBS construction given in Eq. (1), we define the  $N$ -gon states by

$$|\psi_i\rangle = U_i|0\rangle \quad \text{with} \quad U_i = R_z^{(i-1)(N-1)/2} \left( \frac{2\pi}{N} \right) R_y(\theta). \quad (7)$$

Pairwise compatibility  $\langle \psi_i | \psi_{i\pm 1} \rangle = 0$  occurs when  $\theta = \theta_N = \arccos \sqrt{\frac{\cos(\pi/N)}{1 + \cos(\pi/N)}}$ . The  $N$ -cycle NC inequality [3,30] reads

$$S_N = \sum_{i=1}^N \langle A_i A_{i+1} \rangle \geq \bar{S}_N^{\text{NC}} = -N + 2. \quad (8)$$

Measurements on the initial state  $|0\rangle$  violate this inequality maximally, leading to

$$S_N \geq \bar{S}_N^{\text{QM}} = \frac{N - 3N \cos(\pi/N)}{1 + \cos(\pi/N)}. \quad (9)$$

Finally, an inequality for the extended witness  $S_N^{(\text{ext})}$  can be derived in full analogy to inequality (4) [6].

In order to make a connection with chained Bell tests [22,31], we use the CF,

$$\text{CF}_N = \frac{S_N - \bar{S}_N^{\text{NC}}}{\bar{S}_N^{\text{NS}} - \bar{S}_N^{\text{NC}}}, \quad (10)$$

to quantify the strength of nonclassical correlations. Here,  $\bar{S}_N^{\text{NS}}$  is the minimum value of  $S_N$  allowed for nonsignaling measurements. For  $N$ -cycle NC inequalities,  $\bar{S}_N^{\text{NS}} = -N$ , which is also the algebraic limit of the expression. When positive, the value of CF quantifies the potential performance of measurement-based quantum computers [10] and can be used to constrain possible extensions of QM [32]. A property of  $N$ -cycle NC inequalities is that  $\text{CF}_N \rightarrow 1$  as  $N \rightarrow \infty$ . In

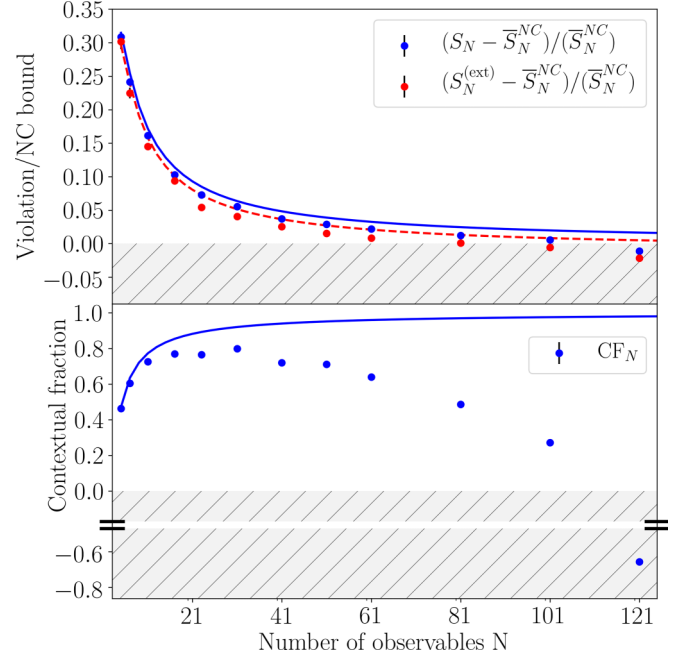


FIG. 4. Results of measurements of  $N$ -cycle witnesses. Solid and dashed lines show QM expectations for relevant quantities (red dashed line includes shot noise), and hashed regions below 0 correspond to results explainable by classical models. The top plot illustrates the fractional gap between quantum and classical witnesses, which decreases for large  $N$ . Our data shows contextuality up to  $N = 101$  ( $N = 61$ ) for  $S_N$  ( $S_N^{(\text{ext})}$ ). The bottom plot shows the calculated contextual fraction. Ideally the system becomes fully contextual at  $N \rightarrow \infty$ , but experimental imperfections lead to  $\text{CF} < 1$  for large enough  $N$ . We measure  $\text{CF}_{31} = 0.800(4)$ . Error bars are generally smaller than the point size.

other words, the system tends to become fully contextual as the number of observables increases. Chained Bell experiments have observed contextuality with  $N$  up to 90, measuring CF as large as  $\text{CF}_{36} = 0.874(1)$  [17]. Here we complement those studies by measuring odd  $N$ -cycle NC inequalities up to  $N = 121$ , while quantifying systematic effects which can compromise experiments on photonic systems [15].

The number of pulses and duration for these experiments both grow as  $N^2$ . In order to shorten the experimental run time we concatenate  $U_j^\dagger U_i$  to  $U_{i-j}$ , rather than performing the full pulse sequence corresponding to  $U_j^\dagger U_i$  [6]. This precludes the blocklike structure of individual measurements [28], but leads to relevant time and infidelity reductions for large  $N$ . All measurements were performed in normal (as opposed to reverse) order, with every correlator measured 10 000 times.

The measurement results are shown in Fig. 4. We identify stronger-than-classical correlations in all prepared scenarios up to  $N = 101$  ( $N = 61$ ) for the bare (extended) witness. Beyond that, our results are consistent with NC models. The largest measured value is  $\text{CF}_{31} = 0.800(4)$ . We have not found a consistent theory model for calculating the CF in the presence of finite signaling, so the plot includes only the results for the bare witnesses. The complete table of results, as well as further experimental details, are available in [6]. These results show contextuality in a system with 101 observables.

Moreover, the measured contextual fraction is larger than in other experiments closing the detection loophole [20].

While QM predicts that  $CF_N$  will approach unity as  $N$  increases, any finite error rate per measurement will cause  $CF_N < 0$  for sufficiently large  $N$ . This is why the experimentally measured values of CF do not grow indefinitely with  $N$ , but rather fall off above  $N = 31$  and eventually become negative. Since  $CF > 0$  certifies quantum advantage, one way to interpret this transition is as classical behavior emerging from a quantum system. While quantum-to-classical transitions are usually considered within the decoherence framework [33], this interpretation cannot be applied here, since measured decoherence in our system occurs over timescales much longer than the duration of our experimental sequences (see [6]). An alternative framework, first proposed in [34], states that quantum-to-classical transitions can occur purely due to measurement fuzziness. Conceptually, as  $N$  grows, different measurement directions can no longer be resolved from one another, leading to results which could have had a classical origin. A previous analysis of Bell inequalities [35] has shown that such a transition toward classicality occurs in an otherwise perfect quantum system if unitary operations are non-ideal, whereas it does not if the final projection is coarsened. Since in our experiment the errors in qutrit rotations dominate over detection errors, we conjecture that we observe the same phenomenon here. Although this effect is also present in previous chained Bell tests [17,20], here the link to quantum-to-classical transitions is discussed in a different context.

The experiments we have performed suggest that nonclassical correlations as strong as predicted by quantum mechanics can be observed in nature. Using this as a starting point, experiments should aim at closing the compatibility loophole without extending the notion of contextuality, which can be accomplished by using multiple entangled qutrits [36]. A further interesting study would be to carry out experiments using the operational definition of contextuality described in [18]. Initial work has already been carried out with photonic systems to study the monogamy relation between contextuality and nonlocality [37], as well as alternative definitions of

contextuality [38]. Comparable experiments on a trapped-ion platform would facilitate closing the detection loophole. Further work is also needed to understand how contextual witnesses measured in the presence of imperfections relate to advantages in computational tasks.

We thank Renato Renner, Ravi Kunjwal, Myungshik Kim, and Hyunseok Jeong for discussions, and Chiara Decaroli for comments on the manuscript. We acknowledge support from the Swiss National Science Foundation under Grant No. 200021 134776. The research is partly based upon work supported by the Office of the Director of National Intelligence (ODNI), Intelligence Advanced Research Projects Activity (IARPA), via the U.S. Army Research Office Grant No. W911NF-16-1-0070. The views and conclusions contained herein are those of the authors and should not be interpreted as necessarily representing the official policies or endorsements, either expressed or implied, of the ODNI, IARPA, or the U.S. Government. The U.S. Government is authorized to reproduce and distribute reprints for Governmental purposes notwithstanding any copyright annotation thereon. Any opinions, findings, and conclusions or recommendations expressed in this material are those of the author(s) and do not necessarily reflect the view of the U.S. Army Research Office. A.C. acknowledges support from Project No. FIS2014-60843-P, “Advanced Quantum Information” (MINECO, Spain), with FEDER funds, the FQXi Large Grant “The Observer Observed: A Bayesian Route to the Reconstruction of Quantum Theory,” and the project “Photonic Quantum Information” (Knut and Alice Wallenberg Foundation, Sweden).

Experimental data were taken by C.Z., M.M., and J.A., using an apparatus primarily built up by F.M.L. and J.A., and with significant contributions from M.M. and C.Z. Data analysis was performed by M.M., J.A., and A.C. The Rapid Communication was written by J.A., M.M., J.P.H., and A.C., with input from all authors. Experiments were conceived by A.C., M.M., J.A., and J.P.H.

The authors declare that they have no competing financial interests.

- 
- [1] S. Kochen and E. P. Specker, in *The Logico-Algebraic Approach to Quantum Mechanics*, The University of Western Ontario Series in Philosophy of Science Vol. 5a, edited by C. A. Hooker (Springer, Dordrecht, 1975), pp. 293–328.
  - [2] P. Heywood and M. L. G. Redhead, *Found. Phys.* **13**, 481 (1983).
  - [3] A. Cabello, S. Severini, and A. Winter, [arXiv:1010.2163](https://arxiv.org/abs/1010.2163).
  - [4] A. A. Klyachko, M. A. Can, S. Binicioğlu, and A. S. Shumovsky, *Phys. Rev. Lett.* **101**, 020403 (2008).
  - [5] A. Cabello, S. Severini, and A. Winter, *Phys. Rev. Lett.* **112**, 040401 (2014).
  - [6] See Supplemental Material at <http://link.aps.org/supplemental/10.1103/PhysRevA.98.050102> for details on experimental procedures and data analysis, theoretical discussions and a comparison with previous NC tests.
  - [7] M. Araújo, M. T. Quintino, C. Budroni, M. T. Cunha, and A. Cabello, *Phys. Rev. A* **88**, 022118 (2013).
  - [8] C. Dhara, G. Pretico, and A. Acín, *Phys. Rev. A* **88**, 052116 (2013).
  - [9] A. Cabello, *Phys. Rev. Lett.* **110**, 060402 (2013).
  - [10] S. Abramsky, R. S. Barbosa, and S. Mansfield, *Phys. Rev. Lett.* **119**, 050504 (2017).
  - [11] B. Hensen, H. Bernien, A. Dréau, A. Reiserer, N. Kalb, M. Blok, J. Ruitenberg, R. Vermeulen, R. Schouten, C. Abellán *et al.*, *Nature (London)* **526**, 682 (2015).
  - [12] M. Giustina, M. A. Versteegh, S. Wengerowsky, J. Handsteiner, A. Hochrainer, K. Phelan, F. Steinlechner, J. Kofler, J.-Å. Larsson, C. Abellán *et al.*, *Phys. Rev. Lett.* **115**, 250401 (2015).
  - [13] L. K. Shalm, E. Meyer-Scott, B. G. Christensen, P. Bierhorst, M. A. Wayne, M. J. Stevens, T. Gerrits, S. Glancy, D. R. Hamel, M. S. Allman *et al.*, *Phys. Rev. Lett.* **115**, 250402 (2015).
  - [14] R. Lapkiewicz, P. Li, C. Schaeff, N. K. Langford, S. Ramelow, M. Wieśniak, and A. Zeilinger, *Nature (London)* **474**, 490 (2011); J. Ahrens, E. Amsellem, A. Cabello, and M. Bourennane, *Sci. Rep.* **3**, 2170 (2013).
  - [15] M. Smania, M. Kleinmann, A. Cabello, and M. Bourennane, [arXiv:1801.05739](https://arxiv.org/abs/1801.05739).

- [16] H. S. Poh, S. K. Joshi, A. Cerè, A. Cabello, and C. Kurtsiefer, *Phys. Rev. Lett.* **115**, 180408 (2015).
- [17] B. G. Christensen, Y.-C. Liang, N. Brunner, N. Gisin, and P. G. Kwiat, *Phys. Rev. X* **5**, 041052 (2015).
- [18] R. W. Spekkens, *Phys. Rev. A* **71**, 052108 (2005); R. Kunjwal and R. W. Spekkens, *ibid.* **97**, 052110 (2018).
- [19] J. V. Kujala, E. N. Dzhafarov, and J.-A. Larsson, *Phys. Rev. Lett.* **115**, 150401 (2015).
- [20] T. R. Tan, Y. Wan, S. Erickson, P. Bierhorst, D. Kienzler, S. Glancy, E. Knill, D. Leibfried, and D. J. Wineland, *Phys. Rev. Lett.* **118**, 130403 (2017).
- [21] M. Arias, G. Cañas, E. S. Gómez, J. F. Barra, G. B. Xavier, G. Lima, V. D'Ambrosio, F. Baccari, F. Sciarrino, and A. Cabello, *Phys. Rev. A* **92**, 032126 (2015).
- [22] S. Abramsky and A. Brandenburger, *New J. Phys.* **13**, 113036 (2011).
- [23] O. Gühne, M. Kleinmann, A. Cabello, J.-Å. Larsson, G. Kirchmair, F. Zähringer, R. Gerritsma, and C. F. Roos, *Phys. Rev. A* **81**, 022121 (2010); J.-Å. Larsson, *J. Phys. A: Math. Theor.* **47**, 424003 (2014).
- [24] F. M. Leupold, M. Malinowski, C. Zhang, A. Cabello, J. Alonso, and J. P. Home, *Phys. Rev. Lett.* **120**, 180401 (2018); J. Alonso, F. M. Leupold, Z. U. Solèr, M. Fadel, M. Marinelli, B. C. Keitch, V. Negnevitsky, and J. P. Home, *Nat. Commun.* **7**, 11243 (2016).
- [25] M. Jerger, Y. Reshitnyk, M. Oppliger, A. Potočnik, M. Mondal, A. Wallraff, K. Goodenough, S. Wehner, K. Juliusson, N. K. Langford *et al.*, *Nat. Commun.* **7**, 12930 (2016).
- [26] A. Kent, *Phys. Rev. Lett.* **83**, 3755 (1999); R. Clifton and A. Kent, *Proc. R. Soc. London, Ser. A* **456**, 2101 (2000); A. Cabello, *Phys. Rev. A* **65**, 052101 (2002); X.-M. Hu, J.-S. Chen, B.-H. Liu, Y. Guo, Y.-F. Huang, Z.-Q. Zhou, Y.-J. Han, C.-F. Li, and G.-C. Guo, *Phys. Rev. Lett.* **117**, 170403 (2016).
- [27] G. Kirchmair, F. Zähringer, R. Gerritsma, M. Kleinmann, O. Gühne, A. Cabello, R. Blatt, and C. F. Roos, *Nature (London)* **460**, 494 (2009).
- [28] A. Cabello, *Phys. Rev. A* **93**, 032102 (2016).
- [29] The complete raw dataset is publicly available from an open repository on <http://www.tiqi.ethz.ch/publications-and-awards/public-datasets.html>.
- [30] Y.-C. Liang, R. W. Spekkens, and H. M. Wiseman, *Phys. Rep.* **506**, 1 (2011).
- [31] M. Sadiq, P. Badziąg, M. Bourennane, and A. Cabello, *Phys. Rev. A* **87**, 012128 (2013).
- [32] E. Amsalem, L. E. Danielsen, A. J. López-Tarrida, J. R. Portillo, M. Bourennane, and A. Cabello, *Phys. Rev. Lett.* **108**, 200405 (2012); R. Colbeck and R. Renner, *Nat. Commun.* **2**, 411 (2011).
- [33] W. H. Zurek, *Phys. Today* **44**(10), 36 (1991).
- [34] J. Kofler and C. Brukner, *Phys. Rev. Lett.* **99**, 180403 (2007).
- [35] H. Jeong, Y. Lim, and M. S. Kim, *Phys. Rev. Lett.* **112**, 010402 (2014).
- [36] A. Cabello and M. T. Cunha, *Phys. Rev. Lett.* **106**, 190401 (2011).
- [37] X. Zhan, X. Zhang, J. Li, Y. Zhang, B. C. Sanders, and P. Xue, *Phys. Rev. Lett.* **116**, 090401 (2016).
- [38] M. D. Mazurek, M. F. Pusey, R. Kunjwal, K. J. Resch, and R. W. Spekkens, *Nat. Commun.* **7**, 11780 (2016).